RADIATION DEFECT-INDUCED LATTICE CONTRACTION OF InP*

C. R. WIE**, T. JONES, T. A. TOMBRELLO, T. VREELAND, JR., F. XIONG, and Z. ZHOU

Divisions of Physics, Mathematics, and Astronomy, 301-38 and
Engineering and Applied Sciences
California Institute of Technology
Pasadena, California 91125

and

G. BURNS and F. H. DACOL

IBM Thomas Watson Research Center
Yorktown Heights, New York 10598

ABSTRACT

We studied the lattice strain induced in the MeV ion bombarded InP crystals and the annealing behaviors of lattice strain, Raman line shift, and linewidth. The lattice spacing for the planes parallel to the surface decreases as a result of irradiation, and amounts to a strain of -0.061% for the (100) face, -0.056% for the (110) face, and -0.050% for the (111) face for 15 MeV Cl bombarded samples to a dose of 1.25E15 ions/cm^2. The negative lattice strain, Raman line shift, and line width completely recover at 450°C, and show a major recovery stage at 250°C - 350°C.

To appear in the Proceedings of the Material Research Society, Boston, MA, December 1986.

---

*Supported in part by the National Science Foundation [DMR84-21119].
**Permanent address: SUNY at Buffalo, Dept. of Electrical & Computer Engineering, Amherst, NY 14260.

ONE OF THE BROWN BAG PREPRINT SERIES
IN BASIC AND APPLIED SCIENCE

February 1987

INTRODUCTION

InP is an important III-V compound for optoelectronic, photovoltaic, high-speed logic, and microwave devices. InP and alloys on InP substrates can be used to fabricate integrated electronic and electro-optic devices on the same chip for high-speed computer and communications applications. In spite of its potential, development of InP technology and the materials study on InP has been less emphasized than GaAs [1]. This is partly due to their similar bandgaps and that fabrication technology is easier for GaAs than for InP.

Reported studies of the radiation-induced defects in InP include identification of P_{In} antisites [2], defect states [3-7], formation and annealing of defects [8] in electron-irradiated samples, deep and shallow levels [9] and photoconductivity [10] in light-ion bombarded InP, and annealing of electron traps in γ-ray irradiated samples [11]. In MeV electron-irradiation studies, Levinson *et al.* found many electron traps with anomalously low introduction rates ($10^{-4} - 10^{-3}$ cm^{-1}) compared with GaAs ($\sim$ 1 cm^{-1}) and GaP ($\sim$ 0.1 cm^{-1}) [4]. Koyama *et al.* measured the introduction rate of a dominant electron trap in γ-ray irradiated samples ($\sim$ 0.05 cm^{-1}), and they attributed the lower introduction rate in the electron-irradiated samples to a simultaneous annealing during the irradiation by beam heating [11].

MeV implantation in III-V compounds is interesting because of its potential applications in device processing for such devices as buried channel CCDs, mixer diodes, vertical FETs, and photodiodes [12]. Other applications include buried isolation layers, buried interconnects, and modifications of optical properties for III-V laser devices. MeV ion implantation also can be used to replace costly and time-consuming epitaxial processing [13]. In view of the above, we studied the effects on structural properties [14-16], and the phonon energy shifts [20,21] in GaAs bulk and epitaxial samples resulting from MeV ion implantation.

In this paper we present the experimental data for MeV ion implanted InP crystals. Lattice strain was measured using the x-ray rocking curve technique for MeV implanted InP (100), InP (110), and InP (111). (A dynamical theory analysis of the x-ray rocking curves for MeV ion bombarded crystals is given in reference [17].) The lattice strain was negative for all three orientations. Thermal annealing results on the x-ray strain, Raman

line shift, and linewidth are reported. The thermal annealing behavior is compared with radiation defect annealing data of MeV electron irradiated InP.

Lattice Contraction of InP due to Defects

The n-type or p-type InP wafers were bombarded at room temperature with 15 MeV chlorine ions with particle current 0.04-0.14 $\mu A/cm^2$ or with 6-8 MeV oxygen ions with particle current 4-8 $\mu A/cm^2$. The ions stop a few microns below the sample surface (*e.g.*, $\sim$ 5 μm for 15 MeV Cl). After a high dose ($\geq 10^{15} cm^{-2}$ for 15 MeV Cl), the first 3-4 μm layer becomes populated with a high concentration of point defects and point defect complexes [14,15].

Rocking curves are shown in Figure 1 for the n-type InP samples bombarded to 1.25E 15 cm^{-2} with 15 MeV Cl ions. The small peaks at 0.0 degree correspond to a reflection from the undamaged region of the crystal beyond the ion range. The larger peaks at the positive angles are due to the strain profile in the ion damaged layer. Shifts of the strain peak to positive angles indicate a decrease in the lattice spacing for planes parallel to the surface, that is, in the direction perpendicular to the surface. This is called the perpendicular strain.

There was no change in the lattice parameter in the direction parallel to the surface, as was the case for other III-V crystals [14,15,18]. It is most surprising that the crystal volume contracts as a result of ion bombardment, unlike other III-V compounds (*e.g.*, GaAs, GaP, and InAs) which expand due to ion damage.

The perpendicular lattice parameter change resulting from the ion irradiation is deduced from the rocking curves in Figure 1 and amounts to a strain of -0.061% for (100), -0.056% for (110), and -0.050% for (111). We believe that the uniform strain depth-profile (as is seen from the symmetric shape of the strain peak) is due to a defect concentration which is nearly constant in the first few micron layer [14,15]. The parallel lattice strain was experimentally found to be approximately zero. Perhaps, the reason is that the surface layer is coherently coupled to the substrate lattice [18]. If the coherent lattice coupling was removed, a uniform defect concentration will result in an isotropic lattice strain is approximately -0.03% for 15 MeV Cl ion bombarded InP. (All the three different orientations give approximately same number, as one expects.)

An InP (100) crystal implanted with 8 MeV oxygen ions to 6E 17 ions/cm^2 was found to have a perpendicular x-ray strain of -0.031%. This is lower than in the Cl ion-bombarded sample. We believe that it is due to the higher oxygen beam current which may induce greater annealing from beam heating.

Isochronal Annealing

Isochronal annealing data for an 8 MeV oxygen implanted InP (100) sample are shown in Figure 2(a). Each point was obtained after a 15 minute anneal. The complete recovery of strain is seen to occur at $\sim 450°C$. A major recovery is observed at $300 - 350°C$. Figure 2(b) shows the annealing behavior of LO phonon energy shift and line width obtained from a 6 MeV oxygen implanted InP (100) to a beam dose of 5E 15 cm^{-2}. A complete recovery occurs at $\sim 450°C$ for Raman line shift and width, and a recovery stage is observed at $230 - 300°C$. A 15 MeV Cl ion-bombarded InP (111) sample (dose = 5E 15 cm^{-2}) showed similar behavior for the LO and TO phonon energy shifts.

Discussion

The lattice parameter of InP was reported to decrease with Zn or S doping and increase with Sn doping [19]. This observation was also correlated with the decrease of dislocation density in InP by Zn or S doping.

The lattice parameters of other MeV ion bombarded III-V compounds (GaAs, GaP, and InAs) were all observed to increase [14,15]. Thus, the lattice parameter decrease of InP resulting from radiation damage is most unexpected. For the impurity doping-induced lattice parameter change in InP, Sugii suggested that the electronegativity difference between host and substituted atoms is more important than the difference in covalent radii. In the MeV ion-bombarded InP, the Coulomb interaction of various charge states of the defect may play an important role in the lattice contraction.

The annealing data imply several interesting points regarding the nature of MeV ion induced defects in InP. First, the defects responsible for the negative strain recover completely by annealing at $450 - 500°C$. This is similar to the case of GaAs where a complete recovery of strain and Raman line shifts occurs at $\sim 500°C$ [15,20]. For III-V compounds, there is a corelation between the Debye temperature and the annealing

temperature of native defects [22]. Since the Debye temperatures of InP and GaAs are very similar [23], the complete-recovery temperature for strain is consistent with Lang's argument [22]. The annealing temperature of Se-implanted amorphous InP (740°C) [24] is also close to the annealing temperature of strain ($\sim$ 700°C) in the heavily damaged region of GaAs around the end of ion range [15]. However, in GaAs the defect annealing begins at the temperatures higher than 200 K [25], while in InP major annealing takes place during the irradiation at 77 K [8]. It has been suggested that the ionization-assisted defect diffusion and the beam heating effect can cause an intensive annealing in InP during irradiation [8,11]. The simultaneous annealing during irradiation is also observed in a higher current, 6-8 MeV oxygen bombarded InP sample, where the magnitude of saturated strain is about a factor of two lower than in the Cl bombarded InP.

It is interesting to compare the major recovery stage of strain and Raman lines at 250 – 350°C to the annealing results of radiation defects in MeV electron irradiated InP [8]. In the electron irradiated n-InP, the conductivty recovered completely by annealing at 320°C for 1-4 MeV, at 540°C for 12-14 MeV, and at 700°C for 50 MeV electron bombardments [8]. The last anneal state (470 – 540°C) in the 14 MeV bombarded sample, which was absent from 1-4 MeV samples, was attributed to more complicated defects created by higher energy electrons. The anneal state III of the conductivity recovery was at higher temperature for higher electron energy, *i.e.*, 230 – 320°C for 1-4 MeV, 270 – 400°C for 12-14 MeV and 290 – 470°C for 50 MeV electron bombardments [8]. Our 250 – 350°C recovery state is close to the stage III in the MeV electron bombarded sample. Moreover, the complete recovery of x-ray strain and Raman lines suggests that the defects responsible for the negative strain in the MeV ion bombarded InP crystals may be similar to those created by 12-14 MeV electron irradiations. Identification of the specific defects which anneal at stage III in the electron bombarded InP might provide a clue as to why the InP lattice parameter decreases under MeV ion irradiation - unlike other III-V compounds.

Opposite behavior of InP and GaAs has been observed in various electrical properties resulting from defects: Fermi level pinning by surface defects [27], electrical compensation by proton bombardment [28], electrical activity of implanted dopants [29], and the concentration of carrier traps above or below half of the band gap in electron bombarded samples

[4,5,26,30]. We also observed this behavior in the structural properties (lattice strain) in the MeV ion bombarded samples.

REFERENCES

1. K. J. Bachman, Ann. Rev. Matr. Sci. **11** 441 (1981)
2. T. A. Kennedy and N. D. Wilsey, Appl. Phys. Lett. **44** 1089 (1984)
3. M. Levinson, H. Temkin, and W. A. Bonner, J. Electr. Matr. **12** 423 (1983)
4. M. Levinson, J. L. Benton, H. Temkin, and L. C. Kimmerling, Appl. Phys. Lett. 40 990 (1982)
5. A. Sibille and J. C. Bourgoin, Appl. Phys. Lett. **41** 956 (1982)
6. K. Ando, M. Yamaguchi, and C. Uemura, J. Appl. Phys. **55** 4444 (1984)
7. M. Yamaguchi, K. Ando, and C. Uemura, J. Appl. Phys. **55** 3160 (1984)
8. E. Yu. Brailovskii, F. K. Karapetyan, I. G. Megela, and V. P. Tartachnik, Phys. Stat. Sol. (a) **71** 563 (1982)
9. A. T. Macrander, B. Schwartz, and M. W. Focht, J. Appl. Phys. **55** 3595 (1984)
10. P. J. Downey and B. Tell, J. Appl. Phys. **56** 2672 (1984)
11. J. Koyama, J. Shirafuji, and Y. Inuishi, Electron. Lett. **19** 609 (1983)
12. H. B. Dietsich in Advanced Applications of Ion Implantation, SPIE Proc. **530** 30 (1985)
13. R. S. Payne, W. N. Grant, and W. J. Bertram, IEDM, Washington, 1980, p. 248
14. C. R. Wie, T. A. Tombrello, and T. Vreeland, Jr., Phys. Rev. **B33** 4083 (1986)
15. C. R. Wie, T. Vreeland, Jr., and T. A. Tombrello, Nucl. Instr. Meth. **B16** 44 (1986)
16. C. R. Wie, Presented at the 9th Conf. on the Appl. of Accelerators in Industry and Reserach, Denton, Texas, Nov. 1986
17. C. R. Wie, T. A. Tombrello, and T. Vreeland, Jr., J. Appl. Phys. **59** 3743 (1986)
18. C. R. Wie, T. Vreeland, Jr., and T. A. Tombrello, Matr. Res. Soc. Symp. Proc. **35** 305 (1985)
19. K. Sugii, H. Koizumi, and E. Kubota, J. Electron. Matr. **12** 701 (1983)

20. G. Burns, F. H. Dacol, C. R. Wie, E. Burstein, and M. Cardona, submitted to Mat. Res. Soc. Symp. 1986, Boston (this conference), and Bull. Am. Phys. Soc. **31** 400 (1986)
21. G. Burns, F. H. Dacol, C. R. Wie, E. Burstein, and M. Cardona, to be published in Solid State Comm.
22. D. V. Lang, R. A. Logan, and L. C. Kimmerling, Phys. Rev. **B15** 4874 (1977)
23. U. Piesbergen in Semiconductors and Semimetals, Vol. 2, ed. by R. K. Willardson and A. C. Beer (Academic Press, NY 1966) p. 49
24. J. D. Woodhouse, J. P. Donnelly, P. M. Nitishin, E. B. Owens and J. L. Ryan, Solid State Electron. **27** 677 (1984)
25. K. Thommen, Rad. Eff. **2** 201 (1970)
26. K. V. Lang, L. C. Kimmerling, and S. Y. Leung, J. Appl. Phys. **47** 3587 (1976)
27. W. B. Spicer, I. Lindau, P. Skeath, C. Y. Su, and P. Chye, Phys. Rev. Lett. **44** 420 (1980) and references therein
28. J. P. Donnelly and F. J. Leonberger, Solid State Electron. **20** 183 (1977)
29. See, for example, J. P. Donnelly, Nucl. Instr. Meth. **B182/183** Part 2, 553 (1981)
30. D. Pons, A. Mircea, and J. Bourgoin, J. Appl. Phys. **51** 4150 (1980)

FIGURE CAPTIONS

Figure 1: The x-ray rocking curves taken with FeKal radiation. The InP crystals were bombarded with 15 MeV Cl ions to 1.25 E 15/cm^2 beam dose at room temperature. The perpendicular strain obtained from these data is discussed in the text.

Figure 2(a): The isochronal anneal data of the negative strain in the MeV ion bombarded InP (100) crystal.

Figure 2(b): The anneal behaviors of the LO phonon shift and linewidth of the MeV bombarded InP (100). The ion was 6 MeV oxygen with beam dose 5E 15 cm^{-2}.

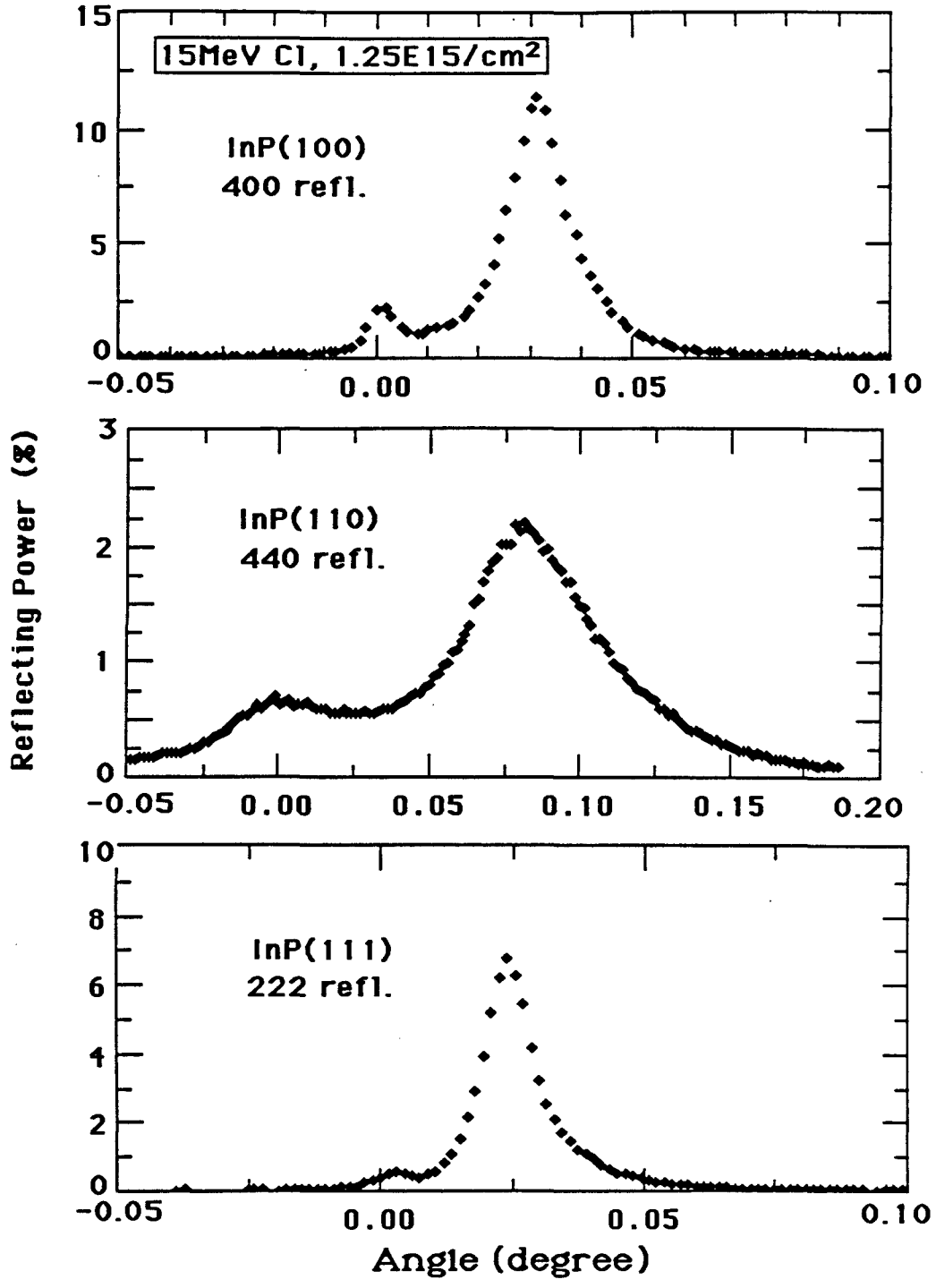
15MeV Cl, 1.25E15/cm²
InP(100)
400 refl.
InP(110)
440 refl.
InP(111)
222 refl.
Reflecting Power (%)
Angle (degree)

Figure 1

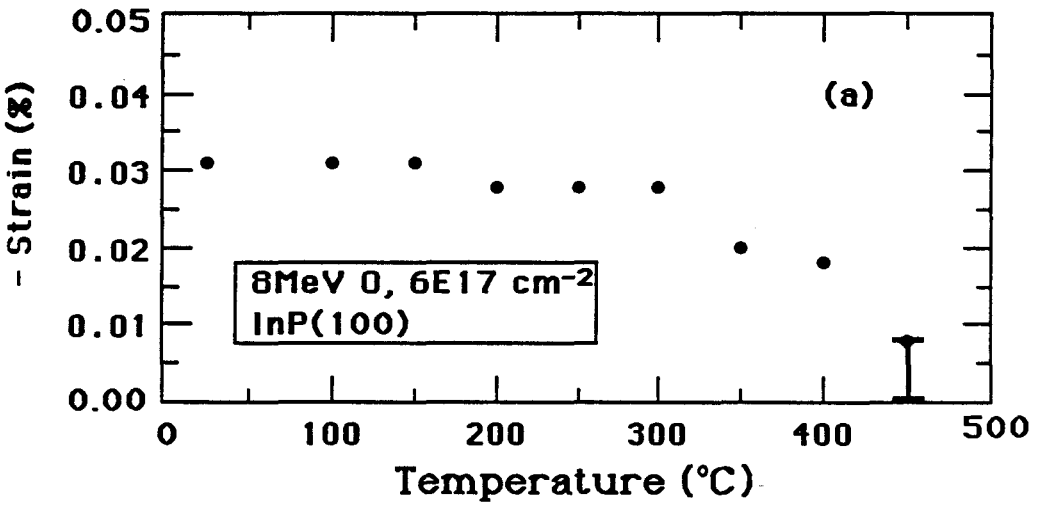
0.05
0.04
0.03
0.02
0.01
0.00
- Strain (%)
(a)
8MeV O, 6E17 cm-2
InP(100)
0
100
200
300
400
500
Temperature (°C)

Figure 2(a)

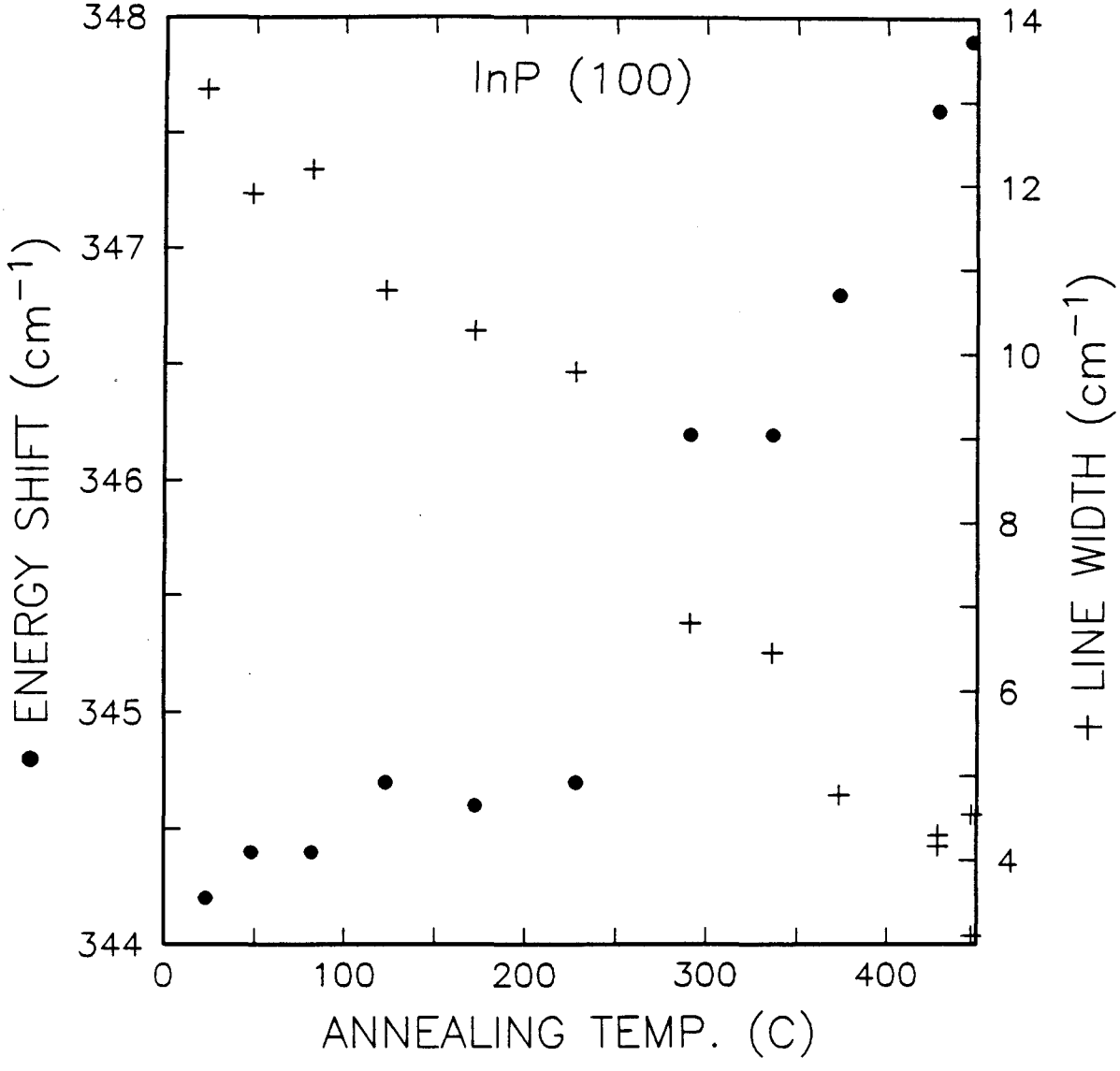
InP (100)
348
347
346
345
344
14
12
10
8
6
4
0
100
200
300
400
ANNEALING TEMP. (C)
• ENERGY SHIFT (cm^{-1})
+ LINE WIDTH (cm^{-1})

Figure 2(b)

BROWN BAG PREPRINT SERIES

BB-37 Liquid Target Generation Techniques in Molecular Dynamics Studies of Sputtering
BB-38 The Measurement of Eolian Sand Ripple Cross-Sectional Shapes
BB-39 Booming Dunes
BB-40 Dynamical Simulations of Granular Materials Using Concurrent Processing Computers
BB-41 A Simulation Study of the Low Energy Ejecta Resulting from Single Impacts in Eolian Saltation
BB-42 Particles in Motion: The Case of the Loaded Die
BB-43 Comparison of Several Nuclear Reaction Techniques for Hydrogen Depth Profiling in Solids
BB-44 Surface Cracking of Vitreous Fused Silica Induced by MeV Ion Beam Bombardment
BB-45 Computer Simulation of the Mechanical Sorting of Grains
BB-46 Feedback in Wind-Blown Sand Transport
BB-47 Scratching the Surface
BB-48 Computing with Particles
BB-49 Faunal Sorting of Sediments: Some Experiments with Desert Beetles Genus (Eleodes)
BB-50 The Impact Process in Eolian Saltation: Two-Dimensional Studies
BB-51 The Ubiquity of C-H Bond Breaking by MeV Ion Irradiation
BB-52 Electrical and Structural Changes in GaAs Crystals from High-Energy, Heavy-Ion Implants
BB-53 Hydrogen Depth Profiling in Solids: A Comparison of Several Resonant Nuclear Reaction Techniques
BB-54 Response of Desert Pavement to Surface Disturbances
BB-55 Simulation Studies of Collision Cascades in Liquid In Targets
BB-56 A Theoretical Model for Eolian Impact Ripples